Resource Management for Macrocell Users in Hybrid Access Femtocells

Elena Bernal-Mor[*†], **Vicent Pla**[*], **David M. Gutierrez-Estevez**[†] and **Jorge Martinez-Bauset**[*]

[*]ITACA Research Institute, Universitat Politècnica de València, (UPV), València 46022, Spain
Email: elbermo@upvnet.upv.es, {vpla; jmartinez}@dcom.upv.es

[†]Broadband Wireless Networking Laboratory
School of Electrical and Computer Engineering, Georgia Institute of Technology, Atlanta, Georgia 30332, USA
Email: david.gutierrez@ece.gatech.edu

***Abstract*—The constant evolution of mobile-phone traffic demands for novel networking solutions especially focused on indoor environment. In this context, the use of femtocells, i.e., cells with very limited coverage area, has been proposed. In this paper, a femtocell network with hybrid access control mode is considered. The activity profile of the Femtocell Users (FUs) is modeled to compute the maximum achievable throughput and the consumed energy per successfully transmitted data bit by the Macrocell Users (MUs), depending on which set of channels are operated in open access mode, i.e., which channels can be used by MUs. Thus, it is identified how many and which channels must be operated in open access mode, depending on the physical capacities of the channels and the amount of time these channels are not occupied by FUs. The results motivate the need for novel resource management schemes which can dynamically adapt the set of open access channels to the network conditions.**

I. Introduction

During the recent years, the high penetration of mobile-phone services into the society has lead to an unprecedented growth in the data-traffic volume. This trend will continue in the coming years, as mobile systems are expected to support a larger variety of multimedia services. Unfortunately, the current networks' features are not enough to face this development paradigm. Moreover, according to recent surveys [1], the traffic which is expected to produce the bulk of the network load will mainly occur indoor. In this context, the novel concept of femtocells [2], [3] has emerged to increase both network capacity and indoor coverage.

Femtocells are small coverage areas, created by low-power base stations called Femtocell Access Points (FAPs) for providing indoor services. They are owned and installed by the users. As a result, users improve their QoS, while operators can manage the growth of traffic without the need to construct new network infrastructures. Moreover, the FAPs send the backhaul data over the Internet to the cellular operator network, thus allowing operators to release resources for other Macro Users (MUs). However, the deployment of femtocells introduces several technical challenges [4].

One of the performance-limiting factors in femtocell deployments is the cross-tier interference between the macrocell and the femtocell [5]. This problem has been widely addressed in the literature and many approaches have been proposed to cope with it, which involve the use of power control [6], [7] or advanced spectrum management techniques [8], [9]. Moreover, the radio interference can be managed by allowing strong macrocell interferers to connect and acquire some level of service in femtocells [10]. A key mechanism for operators to provide different levels of priority to Femtocell Users (FUs) and MUs is the Access Control (AC) policy, which is the protocol that regulates the access of the users to a femtocell. For this, three access control modes exist [11]: i) a *closed* access mode where the femtocell resources can be used only for FUs; ii) an *open* access mode where all the femtocell resources are available for MUs; and iii) a *hybrid* access mode where MUs can only access a limited number of femtocell resources.

Several studies can be found in the literature which compare open and closed access modes for femtocell networks [12], [13]. On the one hand, in the open access mode, the number of dropped sessions due to cross-tier interference between macrocells and femtocells can be reduced by allowing the most harmful interfering MUs to connect to the femtocell. On the other hand, the closed access mode does not entail security and sharing concerns, and it is more preferred by femtocell customers because they own and install the FAPs in their private environments. The hybrid access mode is proposed [14], [15] as a trade-off between open and closed access modes where the access control has to be carefully chosen depending on the scenario under study and the customer profile.

In this paper, we develop an analytical model of the FU activity profile to study which channels are the best to be operated in open access mode. Our model assumes that the FUs have priority over the MUs since the femtocell customers are the owners of the FAPs. In our study, if an MU is connected to the femtocell while an FU is in need of the resources used by the MU, the MU will vacate the channel. To the best of our knowledge, this priority of FUs is not considered in existing works. The study of the hybrid access mode proposed in this paper allows to identify which channels are the best option for MUs depending on the Signal to Interference Noise Ratio (SINR) experienced by the users on each channel and the

978-1-4673-0921-9/12/$31.00

amount of time an FU is using these channels. The results motivate the need for novel resource management schemes which dynamically adapt the set of channels operating open access mode depending on the network conditions.

The remainder of this paper is organized as follows. In Section II, we describe the system model to study the activity profile of FUs. In Section III, we derive expressions for several performance parameters for MUs from the model in Section II. In Section IV, we discuss and compare the numerical results. Finally, Section V concludes the paper.

II. FU ACTIVITY PROFILE MODEL

In this section, we present a model of the FU activity profile. We consider a single femtocell with C available channels, from which $C_m \leq C$ are operating Open Access (OA) mode. Each channel experiences different signal and interference levels and therefore the data rate achieved in each channel is different. The data rate on channel i is R_i bit/second. We consider that one specific channel has the same average radio characteristics, e.g., SINR, for all users (FUs and MUs) and which are static during the period of time under consideration.

The traffic can be mainly classified in two different types, namely, elastic traffic and streaming traffic [16]. *Elastic traffic* corresponds to the transfer of digital documents.*Streaming traffic* corresponds to real-time services. In case of elastic traffic, the session duration depends on the data rate received. High data rates entail shorter session durations. In case of streaming traffic, the session duration only depends on the user behavior. We consider that FUs generate streaming traffic, but the model could be extended to the case of elastic traffic.

A. System Model

We model the activity profile of FUs using a multidimensional Continuous-Time Markov Chain (CTMC), which is shown in Fig.1. The system state vector $\boldsymbol{x}$ is described by the C-tuple $\boldsymbol{x} = (x_1, \ldots, x_C)$, where x_i takes value 0 when the channel i is idle and 1 when it is used by an FU (busy). We consider that one FU session uses one channel, therefore the number of FUs connected to the femtocell at state $\boldsymbol{x}$ is represented by $N(\boldsymbol{x}) = \sum_{i=1}^{i=C} x_i$.

We consider a finite user population with M FUs. The arrival rate λ at state $\boldsymbol{x}$ is given by:

$$\lambda(\boldsymbol{x}) = (M - N(\boldsymbol{x}))\lambda_f \quad (1)$$

where λ_f refers to the arrival rate for one iddle FU.

Incoming FUs access the channels by following an order, namely, the FUs access the channels by choosing the most preferred channel among all the available idle channels. The most preferred channel ($i = 1$) is the channel having the highest data rate, while the least preferred channel ($i = C$) is the channel having the lowest data rate. If there are no idle channels, i.e., all of them are occupied by FUs, an incoming FU is blocked out of the femtocell. For the sake of mathematical tractability, we consider exponentially distributed session durations for FUs, and $1/\mu$ is the average session duration.

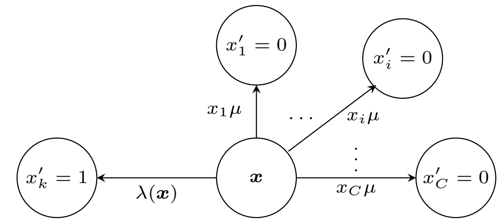

Fig. 1. State transitions of the CTMC which model the FU activity profile.

We consider that MUs generate packets with a fixed size $L = L_H + L_D$ bits, where L_H and L_D are, respectively, the header and payload lengths. The MUs use the channels operated in OA mode not used by FU traffic. We consider that the MUs are in saturation, i.e., there are always MUs waiting for free channels. Therefore, for this study, it is not relevant which channels the MUs choose first when they access the femtocell. Upon an FU arrival, MUs vacate the channel chosen by the FU and the MU packet that is being transmitted is lost, i.e., we consider a preemptive and non-resume access control policy. Thus, when the MUs access a higher number of preferred channels, MU transmissions are more likely to be interrupted. It is under study in this work, how many channels and which channels are assigned as OA mode to MUs.

The state transitions of the CTMC under study occur when a new FU session connects to the femtocell or when any FU session is finished. The state $\boldsymbol{x'}$ represents the state achieved by the femtocell after a state transition and $q_{xx'}$ is the transition rate from $\boldsymbol{x}$ to $\boldsymbol{x'}$. The transition matrix $\boldsymbol{Q}$ when the states are lexicographically sorted can be easily obtained by using the $q_{xx'}$. This is shown in Fig. 1. The channel states from $\boldsymbol{x'}$ that are not represented in Fig. 1 keep the same status as in $\boldsymbol{x}$ and the kth channel is the channel with $k = \min\{(i) \mid x_i = 0\}$. Note that in state $\boldsymbol{x}$ only one transition can occur due to an arrival of an FU, while up to $N(\boldsymbol{x})$ different transitions can occur when an FU finishes its service. Let $\boldsymbol{\pi}$ denote the vector of stationary probabilities obtained by using the global balance equations and the normalization equation given by:

$$\pi(\boldsymbol{x}) \sum_{\forall \boldsymbol{x} \neq \boldsymbol{x'}} q_{xx'} = \sum_{\forall \boldsymbol{x'} \neq \boldsymbol{x}} q_{x'x} \pi(\boldsymbol{x'}); \quad \sum_{\forall \boldsymbol{x}} \pi(\boldsymbol{x}) = 1. \quad (2)$$

B. Characterization of Idle and Busy Periods

Our goal is to characterize the time intervals when an arbitrary channel is used by an FU (busy period, B_i) and the time intervals when an arbitrary channel is not used by any FU (idle period, I_i). Therefore, the busy period B_i corresponds to the channel holding time of FUs in channel i, which is exponentially distributed with rate μ $\forall i$. The idle period I_i corresponds to the period of time spent in the set of states with $x_i = 0$. Hence, the idle period follows a phase type distribution, which defines the time until absorption ($x_i \to 1$) in an Absorbing Markov Process (AMP) [17] and it is represented by $PH(\boldsymbol{\alpha}, \boldsymbol{S})$, where $\boldsymbol{S}$ is the transition matrix which conteins the transition rates between the states and $\boldsymbol{\alpha}$ is the initial state probability vector.

For each channel i, a different AMP is defined $PH(\boldsymbol{\alpha}_i, \boldsymbol{S}_i)$. The AMP is initiated when channel i becomes idle and the absorption occurs when it becomes busy. Therefore, the matrix $\boldsymbol{S}_i$ is obtained from $\boldsymbol{Q}$ by removing the rows and the columns corresponding to the states where channel i is busy. The probabilities $\boldsymbol{\alpha}_i$ are the normalized probabilities of initiating the process at each of the states where $x_i = 0$, given by:

$$\boldsymbol{\alpha_i} = \frac{1}{\sum\limits_{\forall \boldsymbol{\pi}_{x_i=1}} \boldsymbol{\pi}_{x_i=1} \boldsymbol{Q}_{x_i=1,x_i'=0}} \boldsymbol{\pi}_{x_i=1} \boldsymbol{Q}_{x_i=1,x_i'=0} \tag{3}$$

where $\boldsymbol{\pi}_{x_i=1}$ is a row vector with the probabilities for the busy states and $\boldsymbol{Q}_{x_i=1,x_i'=0}$ is a matrix with transition rates from busy states to idle states.

The cumulative distribution function corresponding to the idle period of channel i is $F_{I_i}(t) = 1 - \boldsymbol{\alpha}_i e^{t\boldsymbol{S}_i} \mathbf{1}$, where $\mathbf{1}$ is the unity vector. The average time in which the channel i is idle corresponds to the mean time until absorption in the $PH(\boldsymbol{\alpha_i}, \boldsymbol{S}_i)$ AMP distribution and it is given by:

$$E[I_i] = -\boldsymbol{\alpha}_i \boldsymbol{S}_i^{-1} \mathbf{1}. \tag{4}$$

III. Performance Metrics for macro users

In this section, we derive the analytical expressions for several performance parameters for MUs, by starting from the model defined in Section II.

The probability that at least n packets of length L, corresponding to nL bits, are transmitted during the idle period I_i of the channel i is:

$$p_i(n) = P\left(I_i \geq \frac{nL}{R_i}\right) = 1 - F_{I_i}\left(\frac{nL}{R_i}\right) = \boldsymbol{\alpha}_i e^{\frac{nL}{R_i}\boldsymbol{S}_i} \mathbf{1} \tag{5}$$

where R_i is the data rate on channel i.

The maximum achievable throughput for MUs in the channel i, γ_i, is defined as the average successfully transmitted data bits during an idle period divided by the total average time of idle plus busy periods. The average number of successfully transmitted data bit in channel i, $\overline{D}_i$, is:

$$\begin{aligned} \overline{D}_i &= L_D \sum_{n=1}^{\infty} p_i(n) = L_D \alpha_i \left(\sum_{n=0}^{\infty} \left(e^{\frac{L}{R_i}\boldsymbol{S}_i} \right)^n - 1 \right) \mathbf{1} \\ &= L_D \alpha_i e^{\frac{L}{R_i}\boldsymbol{S}_i} \left(\boldsymbol{I} - e^{\frac{L}{R_i}\boldsymbol{S}_i} \right)^{-1} \mathbf{1} \end{aligned} \tag{6}$$

where $\boldsymbol{I}$ is the identity matrix and L_D refers to the payload length. From (4), (6) and knowing that the busy period B_i is exponentially distributed with mean $1/\mu$, the throughput γ_i for the channel i is given by:

$$\gamma_i = \frac{\overline{D}_i}{\overline{I}_i + \overline{B}_i} = \frac{L_D \alpha_i e^{\frac{L}{R_i}\boldsymbol{S}_i} \left(\boldsymbol{I} - e^{\frac{L}{R_i}\boldsymbol{S}_i} \right)^{-1} \mathbf{1}}{-\boldsymbol{\alpha}_i \boldsymbol{S}_i^{-1} \mathbf{1} + 1/\mu}. \tag{7}$$

The total achievable throughput is the sum of the achievable throughputs in the C_m channels operated in OA mode,

$$\gamma_T = \sum_{\forall i \in OA} \gamma_i. \tag{8}$$

During an idle period of time there are $\Phi_i = D_i/L_D$ successfully transmitted packets on the channel i and one packet interrupted by an FU arrival. The probability that an MU packet is interrupted on the channel i is $\xi_i = 1/(\overline{\Phi}_i + 1)$ and the number of transmitted packets per time unit on the channel i is $(\overline{\Phi}_i + 1)/(\overline{I}_i + \overline{B}_i)$. Therefore, the global MU interruption probability ξ_G is obtained by dividing the sum of interrupted transmissions per time unit of each channel operated in OA mode by the total transmissions per time unit in the same channels. This is given by:

$$\begin{aligned} \xi_G &= \frac{1}{\sum\limits_{\forall j \in OA} \frac{\overline{\Phi}_j + 1}{\overline{I}_j + \overline{B}_j}} \sum_{\forall k \in OA} \frac{\overline{\Phi}_k + 1}{\overline{I}_k + \overline{B}_k} \xi_k \\ &= \frac{\sum\limits_{\forall k \in OA} \frac{1}{-\boldsymbol{\alpha}_k \boldsymbol{S}_k^{-1} \mathbf{1} + 1/\mu}}{\frac{\gamma_T}{L_D} + \sum\limits_{\forall j \in OA} \frac{1}{-\boldsymbol{\alpha}_j \boldsymbol{S}_j^{-1} \mathbf{1} + 1/\mu}}. \end{aligned} \tag{9}$$

Finally, the consumed energy per successfully transmitted data bit on the channel i for MUs, Eb_i, is computed as the energy consumed by the MUs when they are transmitting plus the energy consumed due to the channel monitoring when channel i is occupied by an FU. The average consumed energy per successfully transmitted data bit, $\overline{Eb}$, results from weighting the average energy consumed $\overline{Eb}_i$ per successfully transmitted data bit on each channel i operated in OA mode by the corresponding fractions of throughput in each channel i. This leads to:

$$\overline{Eb}_i = \frac{P_{TX}\overline{I}_i + P_s \overline{B}_i}{L_D \overline{\Phi}_i} \quad ; \qquad \overline{Eb} = \sum_{\forall i \in OA} \frac{\gamma_i}{\gamma_T} \overline{Eb}_i \tag{10}$$

where P_{TX} is the FAP average transmission power, P_s is the average power consumed to monitor which channels are occupied by FUs, L_D stands for the payload length and Φ_i refers to the successfully transmitted packets in channel i.

IV. Performance evaluation

A. Parameter Setting

In this section, we define the values of the parameters considered in the model. In commercial systems such as Long Term Evolution (LTE), Orthogonal Frequency-Division Multiple Access (OFDMA) is used. The frequency domain is divided into non-overlapping subchannels which occupy a bandwidth of 180kHz. The time domain is divided into slots of 1ms. These subdivisions in time and frequency referred to as Resource Blocks (RBs), are the smallest time-frequency units that can be assigned to an user and correspond to a set of twelve adjacent subcarriers and seven OFDM symbols [18].

As previously pointed out, each channel experiences different SINR levels and therefore the data rate achieved for the MUs in each channel is considered to be different for each channel. In Table I, the different data rates per RB are detailed depending on the experienced SINR levels [19]. Each

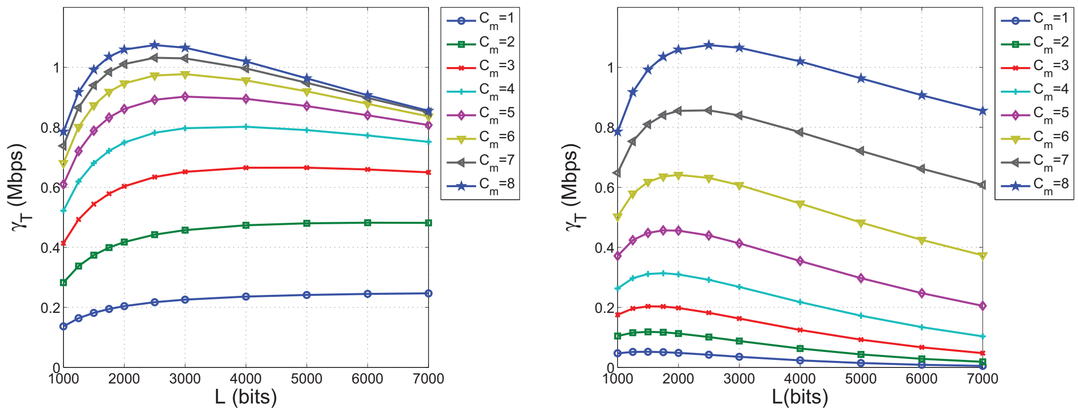

(a) Open access channels with the lowest data rates

(b) Open access channels with the highest data rates

Fig. 2. Maximum achievable throughput γ_T in Mbps for MU vs. L for different sets of open channels operated in OA mode.

RB corresponds here to one channel. We consider a femtocell with $C = 8$ channels. Unless otherwise stated, the data rates achieved by each of the 8 channels are chosen from table I by considering the channels with the best data rate, i.e. $R_1 = 792$ kbit/s, $R_2 = 715.96$ kbit/s $\ldots$ $R_8 = 282.26$ kbit/s.

TABLE I
BITRATES ACHIEVED PER RB AS FUNCTION OF THE SINR [19]

#	SINR (dB)	R_i (in kbit/s/RB)
1	SINR ≥ 22.05	792.00
2	$19.91 \leq$ SINR < 22.05	715.96
3	$17.78 \leq$ SINR < 19.91	640.30
4	$15.64 \leq$ SINR < 17.78	565.27
5	$13.50 \leq$ SINR < 15.64	491.22
6	$11.37 \leq$ SINR < 13.50	418.75
7	$9.23 \leq$ SINR < 11.37	348.69
8	$7.09 \leq$ SINR < 9.23	282.26
9	$4.96 \leq$ SINR < 7.09	221.00
10	$2.82 \leq$ SINR < 4.96	166.64
11	$0.68 \leq$ SINR < 2.82	120.73
12	$-1.45 \leq$ SINR < 0.68	84.09
13	$-3.59 \leq$ SINR < -1.45	56.54
14	$-5.73 \leq$ SINR < -3.59	36.93
15	$-7.86 \leq$ SINR < -5.73	23.60
16	$-10 \leq$ SINR < -7.86	14.85
17	$SINR < -10$	0.00

Since we consider a system with finite population, the offered FU traffic (in Erlangs) to the system is given by:

$$\rho_f = \frac{M}{C} \frac{1/\mu}{1/\lambda_f + 1/\mu} = \frac{M}{C} \frac{\lambda_f}{\lambda_f + \mu}. \quad (11)$$

Unless otherwise stated, the arrival rate per idle FU is chosen to be $\lambda_f = 100\ s^{-1}$, the average channel holding time is $1/\mu = 10$ ms, the packet header length is $L_H = 500$ bits and the total packet size is $L = 4$ kbits. The FU population is $M = 8$. The offered FU traffic as function of these values is $\rho_f = 0.5$. The FAP average transmission power is $P_{TX} = 10$ dBm and the average transmission power consumed to monitor which channels are occupied by FUs is $P_s = 0$ dBm.

B. Numerical Results

In this section, we compare the MU maximum achievable throughput and the interruption probability obtained when the channels operated in OA mode have the highest data rate, i.e. $i = 1, \ldots, C_m$ and when they have the lowest data rate, i.e. $i = C + 1 - C_m, \ldots, C$.

1) Dependence on the packet size:

In Figure 2, the MU maximum achievable throughput γ_T in (8) is shown as a function of the packet size L. We can see that for the same value of channels operated in OA mode C_m, higher throughputs are achieved when the OA channels have the lowest data rate (Fig. 2(a)) than when they have the highest data rate (Fig. 2(b)). This can be explained as follows. The FUs use first the channels with the highest data rate and therefore there are more interruptions which reduce the contribution of these channels to the total throughput, despite having higher data rates. When C_m is small and the OA channels are the channels with the lowest data rates (Fig. 2(a)), having one more OA channel leads to higher gains. When C_m is high, the gain of having one more OA channel is smaller because this channel is used by an FU with a higher probability. This effect is more significant for high L as longer MU packets experience more interruptions. The opposite occurs when the OA channels have the highest data rate (Fig. 2(b)). Regarding the influence of the packet size, the achievable throughput has a maximum for a given L. This is due to the fact that for a smaller packet size L, more header information is transmitted, and for longer packet size L, there are more interruptions.

The interruption probability ϵ_G in (9) is shown in Fig. 3. It can be clearly seen that when the OA channels are the channels with the highest data rate (Fig 3(b)) the interruption probability ϵ_G is higher than when the channels with the lowest data rate are chosen (Fig. 3(a)). This happens because the FUs use first the channels with the highest data rate.

2) Dependence on the data rate achieved by RB:

In Figure 4, results considering different sets of data rates for each channel are shown. We consider $R^{(1)}$ as the set of data rates defined in Section IV-A and $R^{(2)}$ are the set of

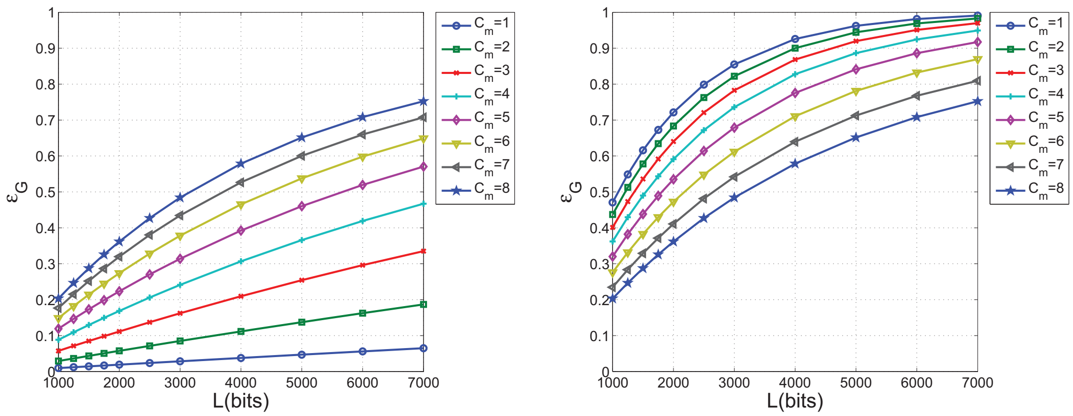

(a) Open access channels with the lowest data rates

(b) Open access channels with the highest data rates

Fig. 3. Interruption probability ϵ_G vs. L for different sets of open channels operated in OA mode.

data rates with values from Table I corresponding to rows $\#1, 3, 5, 7, 10, 12, 14$ and 16 . We have $R_8^{(1)} = 0.356 R_1^{(1)}$ and $R_8^{(2)} = 0.019 R_1^{(2)}$. For $R^{(1)}$, it is better to operate in OA mode the channels with the lowest data rate. However, for $R^{(2)}$, the channels with the highest data rate yield better performance. This can be explained as follows. When the difference of data rates among channels is significant, the data rate achieved in the worst channels is too small, and it is better to access the best channels with higher data rates, despite having more interruptions.

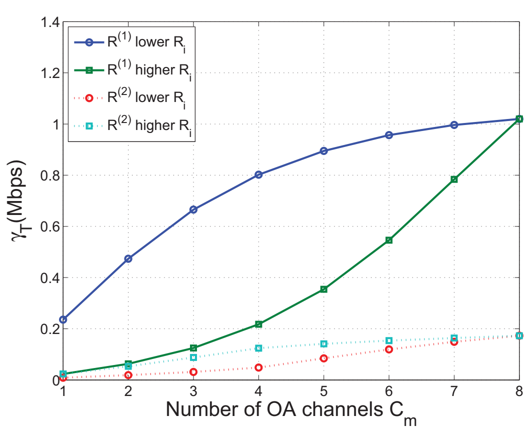

Fig. 4. Maximum achievable throughput γ_T in Mbps for MU vs. C_m for different sets of data rates $R^{(1)}$ and $R^{(2)}$.

When the set of channels operated in OA mode have the highest data rate, the performance only has better results when the difference of data rates among channels is very significant ($R^{(2)}$). Since common scenarios does not present these asymmetrical data rates, from now on $R^{(1)}$ is considered, and the set of channels operated in OA mode are considered to be the channels with the lowest data rate.

3) Dependence on the session duration:

In Figure 5, we show the maximum achievable throughput γ_T for MUs in (8) for different session durations while the offered traffic to the system ρ_f in (11) is kept constant. For small μ the FUs are using the same channel for longer time. This happens because the system varies more slowly, there are less interruptions and therefore, the γ_T is higher. The opposite effect can be seen for high μ. This is because the FUs are using and releasing channels faster, the MUs experience more interruptions and therefore γ_T is lower. It can be seen that the number of C_m channels reaches a point at which considering one more channel operated in OA mode does not contribute to increase in the throughput γ_T. This happens because the best channels are occupied and released continuously by the FUs, thus making these channels useless for MUs.

4) Consumed energy per transmitted data bit:

In Figure 6, the average consumed energy $\overline{Eb}$ per successfully transmitted data bit for MUs in (10) is shown. We can see that given a number of channels operated in OA mode C_m, there is a value of L which makes the $\overline{Eb}$ minimum. This happens because when small packet sizes L are considered, more energy is consumed by the header bits. On the other hand, when long L is considered, more interruptions and more energy is consumed by bits of packets that are not successfully transmitted. Note that the values of L which make the $\overline{Eb}$ minimum are close to the values of L for which the γ_T is maximum, as shown in Fig. 2(a). Regarding the influence of the number of channels operated in OA mode C_m, given a value of L, the value of $\overline{Eb}$ first decreases with C_m, reaches a minimum and then increases again. This happens because for small C_m, the transmission of a bit takes longer since the OA channels have low data rates. For high C_m, more interruptions occur and more power is wasted, despite having high data rates.

V. CONCLUSIONS

In this paper, we study a hybrid access control mode in femtocell networks. We consider a preemptive and non-resume access control policy for the MUs. Different data rates for each channel are considered depending on the SINR experienced by the users. We assess several performance parameters for MUs

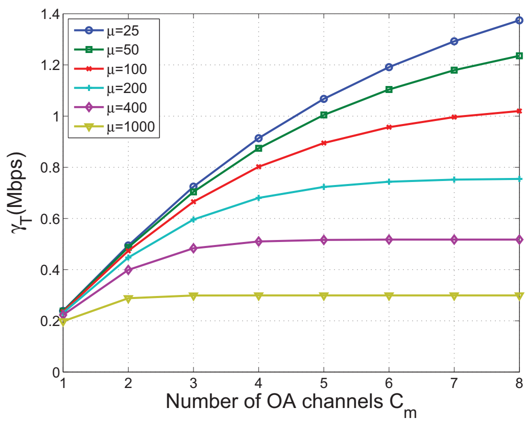

Fig. 5. Maximum achievable throughput γ_T in Mbps for MU vs. C_m for different μ.

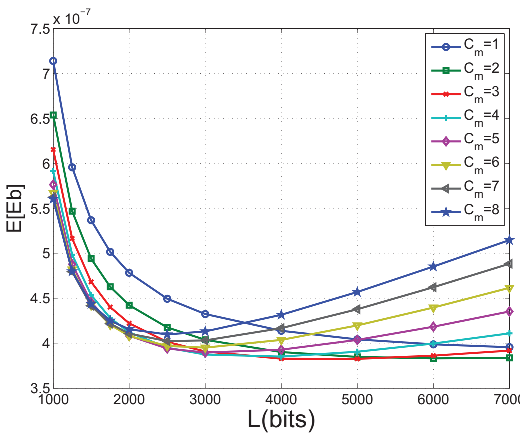

Fig. 6. Consumed energy per successfully transmitted data bit $\overline{Eb}$ (J/bit) vs. L for different C_m.

and we compute how many channels and which channels are the best channels to be operated in open access mode.

The results show that, if the SINR levels experienced by the users in each channel are comparable, the best channels to be operated in OA are the channels with the lowest data rates. Otherwise, if the SINR achieved by the best channels are significantly higher than for the worst channels, it is better to operate the channels with the highest data rates in OA mode. In addition, we show that there is an optimal packet size for MU packets which maximizes the throughput and minimizes the average consumed energy per successfully transmitted data bit. We also demonstrate that for short session durations, the number of channels operated in OA reaches a point at which having more channels operated in OA do not entail any gain to the MU throughput. These results motivate the need for novel resource management schemes which can dynamically adapt the set of OA channels to the channel and network conditions.

ACKNOWLEDGMENT

This research has been funded in part by the European Commission under the FP7 S2EuNet project, the Spanish Government under Project TIN2010-21378-C02-02, and Fundación Caja Madrid. It was completed during the stay of Elena Bernal-Mor at the Broadband Wireless Networking Lab. The authors would like to thank Dr. Ian F. Akyildiz for his valuable comments that improved the quality of this paper.

REFERENCES

[1] G. Mansfield, "Femtocells in the US market-business drivers and consumer proposition," FemtoCells Europe, ATT, London, U.K., Tech. Rep., Jun. 2008.

[2] I. F. Akyildiz, D. M. Gutierrez-Estevez, and E. Chavarria-Reyes, "The evolution to 4G cellular systems: LTE-Advanced," *Physical Communications (Elsevier) Journal*, vol. 3, no. 4, pp. 217–244, December 2010.

[3] V. Chandrasekhar and J. G. Andrews, "Femtocell networks: A survey," *IEEE Communications Magazine*, vol. 46, pp. 59–67, 2008.

[4] D. Lopez-Perez, A. Valcarce, G. de la Roche, and J. Zhang, "OFDMA femtocells. A roadmap on interference avoidance," *IEEE Communications Magazine*, vol. 47, pp. 41–48, 2009.

[5] H. Claussen, "Performance of macro-and co-channel femtocell in a hierarchical cell structure," in *IEEE 18th international Symposium on Personal, Indoor and Mobile Rdio Communications*, Athens, Greece, September 2007, pp. 1–5.

[6] H.-S. Jo, C. Mun, J. Moon, and J.-G. Yook, "Interference mitigation using uplink power control for two-tier femtocell networks," *IEEE Transactions on Wireless Communications*, vol. 8, no. 10, pp. 4906–4910, October 2009.

[7] X. Li, L. Qian, and D. Kataria, "Downlink power control in co-channel macrocell femtocell overlay," in *Proceeding of the 43rd annual conference on Information Sciences and Systems*, Baltimore, MD, March 2009, pp. 383–388.

[8] V. Chandrasekhar and J. Andrews, "Spectrum allocation in tiered cellular networks," *IEEE Transactions on Communications*, vol. 57, no. 10, pp. 3059–3068, October 2009.

[9] N. Saquib, E. Hossain, L. B. Le, and D. I. Kim, "Interference management in OFDMA femtocell networks: Issues and approaches," *IEEE Wireless Communications*.

[10] G. de la Roche, A. Valcarce, D. Lopez-Perez, and J. Zhang, "Access control mechanisms for femtocells," *IEEE Communications Magazine*, vol. 48, no. 1, pp. 33–39, January 2010.

[11] A. Golaop, M. Mustapha, and L. B. Patanapongpibul, "Femtocell access control strategy in UMTS and LTE," *IEEE Communications Magazine*, vol. 47, no. 9, pp. 117–123, September 2009.

[12] Nortel and Vodafone, "Open and closed access for home nodeBs," 3GPP TSG-RAN WG 4(Radio), Athens, Greece, Tech. Rep., Aug. 2007.

[13] P. Xia, V. Chandrasekhar, and J. G. Andrews, "Femtocell access control in the TDMA/OFDMA uplink," in *IEEE GLOBECOM 2010*, Miami, FL, December 2010, pp. 1–5.

[14] D. Das and V. Ramaswamy, "Co-channel femtocell-macrocell deployments - access control," in *IEEE 70th Vehicular Technology Conference Fall (VTC 2009-Fall)*, Anchorage, AK, September 2009, pp. 1–6.

[15] Y.-Y. Li, L. Yen, and E. Sousa, "Hybrid user access control in HSDPA femtocells," in *IEEE GLOBECOM 2010*, Miami, FL, December 2010, pp. 679–683.

[16] T. Bonald and J. Roberts, "Congestion at flow level and the impact of user behaviour," *Computer Networks*, vol. 42, pp. 521–536, 2003.

[17] M. Neuts, *Matrix-geometric Solutions in Stochastic Models: An Algorithmic Approach*. The Johns Hopkins University Press, 1981.

[18] Nortel and Vodafone, "TS 36.211: Physical channels and modulation (release 8)," 3rd Generation Partnership Project, Tech. Rep., 2008.

[19] H. van den Berg, I. Fernandez-Diaz, R. Litjens, K. Spaey, and E. U. Warriach, "Self-optimisation methods for stand-alone functionalities in wireless access networks: Packet Scheduling parameter optimisation," INFSO-ICT-216284 SOCRATES,D3.1B, Tech. Rep., 2009.